Resonance Energy Transfer in Heterogeneous Planar and Bilayer Systems: Theory and Simulation

Luís M. S. Loura*,†,‡ and Manuel Prieto†

Centro de Química-Física Molecular, Instituto Superior Técnico, P-1049-001 Lisboa, Portugal, and Departamento de Química, Universidade de Évora, Rua Romão Ramalho, 59, P-7000-671 Évora, Portugal

Received: January 20, 2000; In Final Form: April 17, 2000

The problem of resonance energy transfer in planar and bilayer geometries with heterogeneous chromophore distributions is studied. Donor fluorescence decays were obtained using the Monte Carlo method for lateral phase separation into continuous and domain phases, and also for probe segregation in linear defects. The generated synthetic curves were analyzed with the mean local concentration model (Liu et al. *Chem. Phys.* **1993**, *177*, 579). It is shown that a significant number of heterogeneity cases can be adequately described by a sum of two Gaussians acceptor concentration distribution. The ability of the analysis method to recover correct acceptor concentration distributions was also tested in more critical conditions, i.e., after convolution of synthetic decay curves and addition of Poisson noise, to emulate experimental fluorescence decay curves. The analysis methodology is shown to be useful to describe probe heterogeneity caused by phase separation, and important parameters (such as the probe partition coefficients) can be recovered.

1. Introduction

Resonance energy transfer (ET) has been a very important tool in biophysical research in the past decades. Most of its applications deal with transfer between donor−acceptor pairs which are all at about the same distance. In this case, ET is used as a "spectroscopic ruler"[1] to determine distances on the nanometer scale.[2] In the case that donor molecules are surrounded by an ensemble of acceptors, the kinetics becomes more complex, and the fluorescence of donor in response to delta-pulse excitation decays nonexponentially. In this article we address the kinetics of ET between chromophores distributed nonrandomly in planar and bilayer geometries. Examples of these kinds of donor−acceptor distributions occur in ET between molecules incorporated in membranes.[3−5] In this work, we show that the methodology used to recover the acceptor concentration distribution function can be used to obtain information on the surface topology (e.g., domain organization) and on the degree of randomness of distribution/aggregation of chromophores. In the following paper[6] the model is applied to common spectroscopic probes in model lipid membranes.

2. Theory of ET in Heterogeneous Media

The time-resolved donor fluorescence intensity in the presence of acceptor, $i_{DA}(t)$, can be described by[7]

$$i_{DA}(t) = A\exp(-t/\tau - C(t/\tau)^{d/6}) \quad (1)$$

where A is a constant, τ is the donor fluorescence lifetime in the absence of acceptor, and d is the dimensionality of the system. For integer dimensionality, C is given by eq 2,[8]

$$C = \Gamma(1 - d/6)n_{dA}V_dR_0^{\,d} \quad (2)$$

Γ being the complete gamma function, n_{dA} the number of acceptors per d-space volume unit (e.g., n_{2A} is the number of acceptors per area unit), V_d is the d-dimensional unit sphere ($V_1 = 2$, $V_2 = \pi$, $V_3 = 4\pi/3$), and R_0 is the Förster radius. This equation has been used to analyze ET data in such diverse media as silica surfaces,[9] porous glasses,[10] Langmuir−Blodgett films,[11,12] and vesicles.[5] The recovery of noninteger d values was usually interpreted on the basis of a fractal structure. However, as first pointed out by Yang et al.[13] and Klafter and Blumen,[14] an "apparent fractal" dimension may be not due to an actual self-similar structure, but either to restricted dimensions of the medium (i.e., nonvalidity of the "infinite medium" assumption[15−18]) or from nonrandom distribution of donors and/or acceptors, contrary to the assumptions made in the deduction of eq 1.[19,20] Due to the ability of the stretched exponential decay function (eq 1, with generally noninteger d) to analyze most decay data (even when there is no physical evidence for noninteger dimensionality), fractal structure was often mistakenly invoked.

When noninteger dimensionality is recovered for systems where the dimensionality of the embedding space is clearly integer, the most common approach (apart from the erroneous fractal interpretation) is to generalize eq 2 by considering that a fraction of the donors (α in the following equation) is isolated, i.e., cannot transfer energy to the acceptors, and has the same decay as in absence of acceptors:[11,12,21]

$$i_{DA}(t) = A[(1 - \alpha)\exp(-t/\tau - C(t/\tau)^{d/6}) + \alpha\exp(-t/\tau)] \quad (3)$$

The physical interpretation is in terms of complete phase separation: strictly, the isolated donors should have no acceptors in their surroundings (that is, closer than $\sim 2R_0$), while all the other donors have the same concentration of randomly distributed acceptors in their vicinity. Of course, this is an extreme situation. In a micro-heterogeneous system, one should expect to find donors with all kinds of surroundings: a few donors would actually be isolated for ET purposes, others would have a given concentration C_1 of acceptors in their surroundings, others still could sense another concentration C_2, and so on.

* Corresponding author. Address: Centro de Química-Física Molecular, Instituto Superior Técnico, P-1049-001 Lisboa, Portugal. Fax: +351 218464455. E-mail: pclloura@alfa.ist.utl.pt.
† Centro de Química-Física Molecular.
‡ Departamento de Química.

10.1021/jp000245y CCC: $19.00
Published on Web 07/01/2000

Liu et al.[22] suggested a formalism which takes into account a continuous probability function $F(C)$ of having donors with a mean local concentration C of acceptors in their surroundings, rather than a discrete function characterized by probability α of seeing no acceptors and probability $1 - \alpha$ of sensing a concentration C, expressed by eq 3. In this model eq 1 is locally valid and the decay law is expressed as a Fredholm integral equation of the first kind regarding recovery of the function $F(C)$:

$$i_{DA}(t) = \int_{C_{min}}^{C_{max}} F(C)\exp(-t/\tau - C(t/\tau)^{d/6})\mathrm{d}C \qquad (4)$$

where C_{min} and C_{max} represent the lower and upper limit values for acceptor concentration, respectively. Of course, in the general case, it should be $C_{min} = 0$ and $C_{max} = +\infty$. However, for numerical integration purposes, C_{max} has to be kept at a finite (but sufficiently large so that $F(C_{max})$ is negligible for $C > C_{max}$) value.

The solution of this equation leads to an ill-conditioned problem, meaning that small errors in $i_{DA}(t)$ may result in large changes in the recovered $F(C)$. Nevertheless, Liu et al. developed a method for distribution analysis without prior assumption of the $F(C)$ curve family, which they tested with computer simulations to largely good results, and applied to the study of diffusion across a polymer interface, ET on the surface of latex microspheres, and dye aggregation in a three-dimensional embedding space. Other applications of the mean local concentration formalism to diffusion in polymers have since then appeared in the literature.[23−25]

However, as first pointed out by Yetka et al.[26] and Farinha et al.,[27] although the mean local concentration model is an improvement over the step-function model expressed by eq 3, in its derivation it is implicitly assumed that each donor is surrounded by a uniform concentration of acceptors. It is therefore not obvious whether it is applicable in the case of spatial nonhomogeneity. This point has also been addressed in later works.[28,29]

Using as starting point the general formalism developed by Klafter and Blumen,[7] Farinha et al. showed that for a planar system in which the distribution function of acceptors is uniform in any thin vertical slice (i.e., the distribution function of acceptors becomes a one-dimensional function), the mean local concentration function (eq 4) is the first term of a converging series expansion.[27] However, even for this simple geometry, the correction term is rather complex, though its weight increases with the Förster radius and the gradient of the distribution function of acceptor. For the case of a planar or bilayer system with domains or fluctuations of probe concentration with spatially uncorrelated locations and varying shapes and sizes, as expected in heterogeneous lipid membranes, the problem seems too complex to be treated analytically.

Therefore, in this work we begin by simulating (using Monte Carlo techniques) the fluorescence decay in a planar system with probe distribution heterogeneity (e.g., coexistence of gel and fluid phases in lipid membranes, each characterized by different acceptor concentrations, and partial probe segregation, e.g., to defect lines of the gel phase lattice) and analyze the synthetic data with the mean local concentration model. In this first section, we intend to establish whether the mean local concentration model is a good approximation in these conditions. In a latter set of simulations, we test our analysis program regarding recovery of concentration distributions in synthetic data in experimental conditions (i.e., after convolution with a typical decay profile and addition of Poisson noise), to check whether the ill-condition of the problem still allows for correct recovery of the model parameters in experimental-like decays.

At variance with Liu et al.,[22] and due to the ill-conditioned problem, we have not tried to recover $F(C)$ in eq 4 without prior assumptions. In this way, for data analysis in this work, we use both unimodal ($h = 0$ in eq 5) and bimodal Gaussian functions to describe $F(C)$:

$$F(C) = A(\exp(-(C - C_1)^2/(2\sigma_1^2)) + h\exp(-(C - C_2)^2/(2\sigma_2^2))) \qquad (5)$$

Gaussian-type functions have been successfully used in the related problems of recovery of lifetime distributions[30] and distance distribution recovery by intramolecular ET.[31−33] Furthermore, the parameters of $F(C)$ (usually a small number) can be treated in the same way as the parameters in a typical decay curve (lifetimes, preexponential ratios), allowing, for example, use of global analysis.[34] In this way, a very large set of functions can in principle be reasonably approximated, by variation of C_1, C_2, σ_1, σ_2, and h, including asymmetric distributions. In particular, a sum of two Gaussian curves should be adequate for analysis of samples in which probes experience two distinct environments, as expected, e.g., for gel/fluid heterogeneity in membranes.

ET in lipid bilayers has two special features which must be taken into account in the analysis procedure. First, the donor usually has a biexponential fluorescence decay curve even in the absence of acceptor. The alterations in the ET decay law that this fact introduces have been described.[20] For homogeneous distribution of acceptor, the decay law becomes

$$i_{DA}(t) = A[\exp(-t/\tau_1 - ct^{d/6}) + q\exp(-t/\tau_2 - ct^{d/6})] \qquad (6)$$

where the subscripts 1 and 2 refer to the lifetime components (τ_1 and τ_2), q is the ratio between the preexponential factors associated with components 2 and 1, and the c parameter is the same for both components (provided that the emission spectra and oscillator strengths of both donor populations are the same) and equals $C/\tau^{1/3}$ for each component.

Second, if (as often is the case, because of slow incorporation kinetics) both acceptor and donor probes have to be mixed with the matrix lipid before hydration, they are distributed along the two leaflets (it is generally assumed that distribution between the leaflets is symmetrical). This is also the case if rapid translocation of probes (flip-flop) between the leaflets occurs, and leads to the following changes in eq 4:

$$i_{DA}(t) = \int_{c_{min}}^{c_{max}} f(c)[\exp(-t/\tau_1) + q\exp(-t/\tau_2)]\rho_c(t,c)\rho_t(t,c)\,dc \qquad (7)$$

where the subscripts c and t refer to transfer either within the same plane (c, cis) or to the opposite plane (t, trans) and the distribution function of the c variable in eq 7 is now denoted f. The cis contribution can be taken into account straightforwardly:

$$\rho_c(t,c) = \exp(-ct^{1/3}) \qquad (8)$$

The trans contribution is more complex:[4]

$$\rho_t(t,c) = \exp\left\{-\frac{2\,c}{\Gamma(^2/_3)b}\int_0^1[1 - \exp(-tb^3\alpha^6)]\alpha^{-3}\mathrm{d}\alpha\right\} \qquad (9)$$

In this equation $b = (R_{0i}/w_i)^2\ \tau_i^{-1/3}$, w_i being the distance between the plane of donors in one leaflet and the plane of the acceptors in the opposite leaflet. If the conditions used to derive

eq 6 are valid, $R_{0i}^2\,\tau_i^{-1/3}$ should be the same for $i = 1,2$.[20] It is also assumed that w_i is the same (or more or less the same) for both donor components, i.e., the complex photophysics is intrinsic to the probes in heterogeneous media, and even if distinct solubilization sites were ascribed to the lifetime components, the difference between their depths in the membrane would be small ($\ll R_0$) and certainly not critical regarding ET (one may thus consider a sole value for b, and a sole ρ_t function).

3. Monte Carlo Generated Decays

Methodology. In the first set of simulations, donors and acceptors were placed in a planar triangular lattice. We chose this model because it resembles the distribution of the lipid polar heads in a gel phase bilayer. Although in fluid bilayers the polar heads are not strictly distributed in such a lattice, as we show in the following paper, heterogeneity is especially pronounced in gel phase bilayers, hence our choice.

The probes are placed in a $10^3 \times 10^3$ lattice (see Figure 1). The bulk concentration of donors is the same for all experiments, i.e., the number of donors ($N_D = 5 \times 10^2$) is constant. As for the number of acceptors, for the first two simulations $N_A = 6.8 \times 10^3$, for the third $N_A = 2 \times 10^3$, for the fourth $N_A = 2 \times 10^4$, and for the fifth $N_A = 4 \times 10^3$. Additional parameters are the donor lifetime ($\tau = 6.5$ ns), and the ratio between the Förster radius and the minimum distance R_e between two molecules ($R_0/R_e = 5.26$, corresponding to (R_0, R_e) pairs of, for example, (50.0 Å, 9.5 Å) or (42.1 Å, 8.0 Å)). For each donor, the decay law is given by[35]

$$\rho_j(t) = \exp\left(-\frac{t}{\tau}\right)\prod_{i=1}^{N_A}\exp\left[\left(-\frac{t}{\tau}\right)\left(\frac{R_0}{R_{ij}}\right)^6\right] \qquad (10)$$

where R_{ij} is the distance between donor j and acceptor i.[36] We assume that there is a single R_0 parameter for every donor−acceptor pair (this condition is met in the dynamic regime) and neglect energy migration among donors (this can be experimentally achieved choosing a donor with no absorption/emission overlap or using low donor concentration). Periodic boundary conditions are used in the calculation of $\rho_j(t)$. The macroscopic decay is obtained by averaging over donors:

$$i_{DA}(t) = \frac{1}{N_D}\sum_{j=1}^{N_D}\rho_j(t) \qquad (11)$$

In previous Monte Carlo studies of ET with heterogeneity of chromophores,[19,36] the distribution heterogeneity was introduced by an interaction potential which reflected the tendency of individual components to self-aggregate or the tendency of different components to be placed nearer than expected for a random distribution. In this work, another approach is considered. We analyze the case of phase separation into domains and linear defects with distinct chromophoric concentrations (see Figure 1).

For simulations 1 and 2, each lattice contains a single square domain at its geometric center with 25% of the total area (a, the area fraction of the domains, is 0.25; see parts 1 and 2 in Figure 1). The donor concentration inside the domains (c_{1D}) is assumed to be equal to that outside (c_{2D}) them (and to the constant bulk concentration c_{bD}). For simulation 1 and 2 we considered $c_{1A} = c_{2A} = c_{bA}$, and $c_{1A} = 2c_{bA} \Rightarrow c_{2A} = (^2/_3)c_{bA}$, respectively, where c_{1A}, c_{2A}, and c_{bA} have the same meaning for the acceptor as c_{1D}, c_{2D}, and c_{bD} for the donor species. In both the domain and outside it, the chromophores are placed randomly, apart from the concentration restrictions given above. As a consequence, the distribution of donor in the whole lattice is always homogeneous (partition constant domain:continuous phase $K_{pD} = 1$). For the acceptor, cases 1 and 2 correspond to homogeneous distribution (partition constant domain:continuous phase $K_{pA} = 1$) and partial segregation into domains ($K_{pA} = 3$), respectively.

For simulations 3−5, we considered a square supramolecular grid (94 molecules wide), with the domains separated by lines (6 molecules wide, $a = 0.12$; see parts 3−5 in Figure 1). Acceptors (and, for simulation 5, also donors) were distributed with different concentrations in the square domains and in the adjacent lines. Even though these lines are not a macroscopic phase, one can still calculate "partition constants" by dividing the probe concentration in the lines (ratio between the probe molecules and the total number of molecules in the lines) by the probe concentration in the squares. K_{pD} (partition constant lines:squares) was unity for simulations 3 and 4. $K_{pD} = 11.4$ and $K_{pA} = 12.7$ was considered for simulation 5. For simulation 3, all 2×10^3 acceptors were put in the lines ($K_{pA} = \infty$). For simulation 4, 2×10^3 acceptors were confined in the lines, and the remaining 1.8×10^4 acceptors were put inside the squares ($K_{pA} = 0.84$; in practice, the acceptor distribution in simulation 4 is obtained from that of simulation 3, adding 1.8×10^4 acceptors to the squares). The simulations were made on a DEC Alphastation 500/400.

The synthetic curves were analyzed in the 10^{-5}−60 ns time range according to eqs 4−5, using nonlinear, least-squares iterative convolution software, based on the Marquardt algorithm.[37] We used three different analysis programs: the program D, which uses discrete acceptor concentration (eq 1); 1G, which uses eq 5, with a Gaussian function for $F(C)$; and 2G, which uses eq 5, with a sum of two Gaussians for $F(C)$. In the analysis procedure, at least 200 subintervals were used to calculate the integrals in eq 7, and C_{max} was always considerably larger than the expected C_{1A} (if, by chance, a recovered distribution extended beyond C_{max}, the analysis was repeated with an increased value for this parameter).

Results. The distributions resulting from the analysis of the time-resolved synthetic data are shown in Figure 2, and the statistical parameters are shown in Table 1. It is clear that for case 1 all programs describe equally well the system. The fitting functions are indistinguishable, and the concentration distributions recovered by the 1G and 2G programs are satisfactory. Program 1G returns a very narrow distribution, while 2G returns two merged (and narrow) Gaussians.

For simulation 2, programs 1G and 2G recover the closest fits. As expected, the parameters recovered by programs D and 1G do not give insight on the acceptor distribution. Program D recovers values close to c_{2A} (the concentration sensed by most donors), slightly shifted to larger abscissas. Program 1G recovers a very broad distribution, with a maximum near c_{2A} but extending into the large c range. On the other hand, the distributions recovered by program 2G compare well with the input c_{1A} and c_{2A} values for each case (see Figure 2, part 2). The estimates of $K_{pA} = c_{2A}/c_{1A}$, $a = (c_{bA} - c_{2A})/(c_{1A} - c_{2A})$, and $K_{pD} = ((1 - a)/a)(I_1/I_2)$ (where I_1 and I_2 are the integrals of the peaks centered at c_{1A} and c_{2A}, respectively), are shown in Table 1 and also agree well with the predicted values. The larger deviations in the recovered K_{pD} values are due to the large error propagation associated with the formula used for its calculation.

In simulations 3−5, the "domain phase" actually consists of linear defects, which are relatively enriched in acceptor and/or

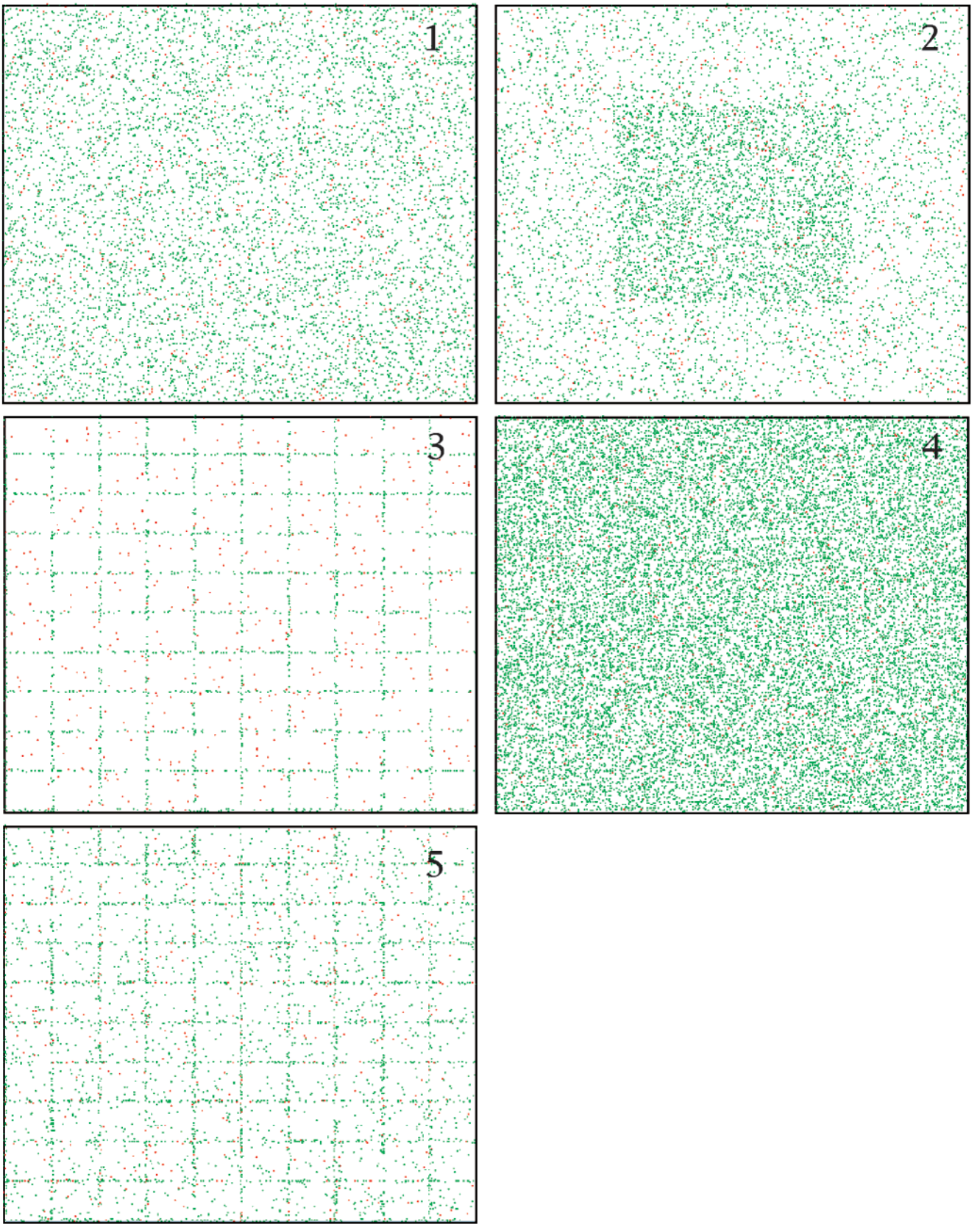

Figure 1. Distributions of donors (red dots) and acceptors (green dots) in the lattice used for the Monte Carlo simulations of ET decays with heterogeneous acceptor distribution. Parts 1−5 correspond to simulations 1−5 in the text (see text for full description). The area of the lattice corresponds to 10^6 molecules. Because of representation limitations, each colored dot occupies the area of approximately 20 molecules. As a result, the chromophore concentrations appear to be larger than the actual values by the same factor.

donor probes (this choice of geometry is relevant for the analysis of the results of the following paper). Again, for simulations 3 and 5, only program 2G returns distributions from which one can obtain meaningful information, and there is a great improvement in χ^2 relative to D or 1G analysis (the latter model recovers tails of Gaussians centered around negative c values).

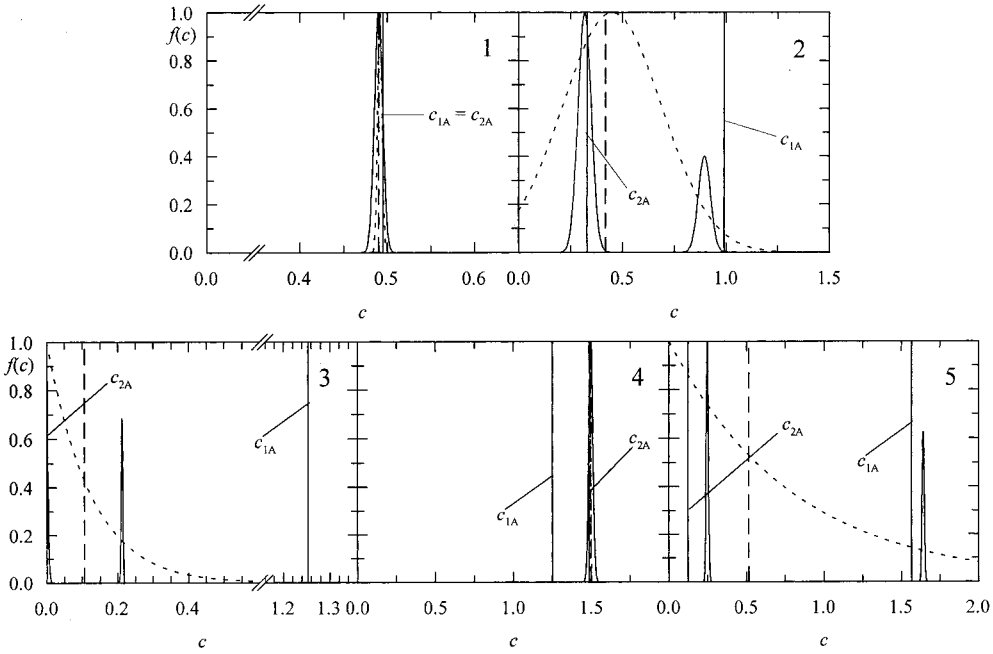

Figure 2. Distributions recovered from the fits to the Monte Carlo generated decays using discrete concentration (D, dashed line), single-Gaussian (1G, dotted line) and sum-of-two-Gaussians (2G, solid line) acceptor concentration distribution models for cases 1−5 (see text and Figure 1). The expected values of centers of distributions c_{1A} and c_{2A} are given for comparison (solid vertical lines, labeled with c_{1A} or c_{2A}). The distribution functions are not normalized in the strict sense, their maximal values were given the value 1.0 for better comparison.

TABLE 1: Statistical Parameters for the Fits of the Different Models to the Monte Carlo Generated Decays[a]

case	1	2	3	4	5
χ^2 (D)/10^{-6}	3.35	26.1	31.5	39.5	727
χ^2 (1G) /10^{-6}	3.18	1.88	3.32	39.5	7.67
χ^2 (2G) /10^{-6}	3.18	1.77	2.74	39.5	3.50
a		0.31(0.25)	0.69(0.12)		0.032(0.12)
K_{pA}	1.0(1.0)	2.8(3.0)	∞(∞)	1.0(0.84)	6.6(12.7)
K_{pD}		0.61(1.0)	0.55(1.0)		19.4(11.4)

[a] D: discrete concentration. 1G: mean local concentration model, Gaussian distribution of acceptors. 2G: mean local concentration model, sum-of-two-Gaussians distribution of acceptors. a: domains' area fraction. K_p: partition coefficient (domains/continuous phase) of Acceptors (K_{PA}) and Donors (K_{PD}), calculated from the 2G fits (predicted values in parentheses).

A predicted domain area fraction value $a = 0.12$ can be calculated by taking into account that those lines have a finite (six-molecule) width. However, this width is small (approximately equal to the assumed R_0 distance), and donors located anywhere on the lines are still sensitive to the environment outside the lines. This is especially important for simulation 3, in which there are no acceptors outside the lines, and donors located at the lines or near them probe a region which is partly loaded with acceptors, and partly depleted of them. The result is that the recovered domain acceptor concentration is much less than the actual value (0.21 instead of 1.25). The fact that a sole peak is recovered for simulation 4 is justified in the same grounds: as the acceptor concentration is similar inside and outside the lines, and given the latter's small width, the 2G program fails to recover a distinct peak resulting from the slightly larger acceptor concentration in the lines. It is therefore not surprising that the values recovered from ET analysis for the domain area fraction a are not accurate. In any case, the K_{pA} and K_{pD} estimates for simulations 3−5 are largely satisfactory (note again that the formulas used for these calculations are subject to serious propagation of uncertainties in c_{1A}, c_{2A}, I_1, and I_2). It should be stressed that reported K_p determinations in membranes are often subject to considerable relative uncertainty. In short, using the 2G program, one is able to obtain the following results:

Simulation 1. Confirmation of distribution homogeneity from recovery of very narrow distributions.

Simulation 2. Detection and characterization of moderate distribution heterogeneity due to differential partition between planar domains.

Specifically for chromophore distribution inside and outside a narrow "linear phase", the following results were obtained.

Simulation 3. Identification of two acceptor concentration peaks, one at $c_{2A} = 0$ (isolated donors, deep in the acceptor-free bulk lattice) and other at $c_{1A} > c_{bA}$ (donors close to or located at the acceptor-rich lines);

Simulation 4. If the previously acceptor-free bulk lattice is loaded with acceptors, so that its local concentration is now similar to that in the lines, recover a sole acceptor concentration peak;

Simulation 5. If there is preferential (but not complete) segregation of both donors and acceptors to the lines, recover two acceptor concentration peaks (but now none located at $c = 0$, because there are acceptors in the bulk), which abscissas and relative intensities allow one to estimate the partition coefficients of the probes.

It is important at this point to stress that in these simulations no noise was introduced. They were meant to test the validity of the mean local concentration model for different kinds of

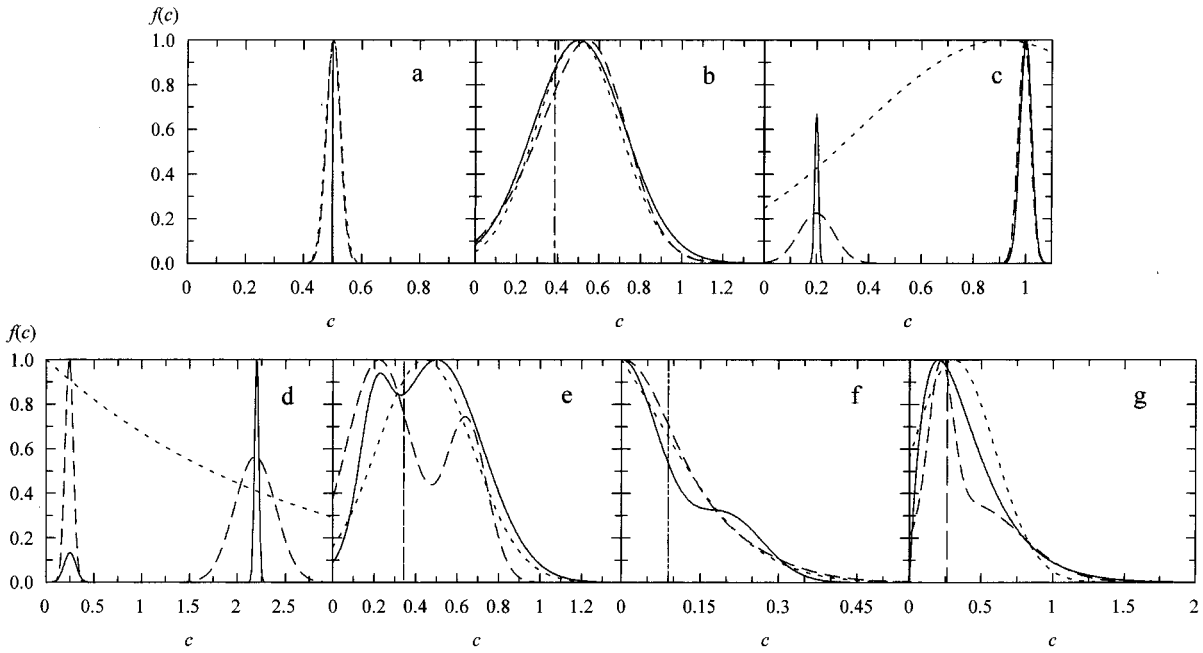

Figure 3. Simulated input acceptor distribution functions (solid lines), and the recovered output functions using programs D (vertical lines; not represented for c and d, because of inability to fit to the data), 1G (dotted curves), and 2G (dashed curves). The letters correspond to the designation given to the synthetic distributions in the text and Table 2. The distribution functions are not normalized in the strict sense, their maximal values were given the value 1.0 for better comparison.

heterogeneity. Concerning this point, they show clearly that the model (in the two Gaussian version) can be used to gain insight on heterogeneous probe distributions. However, due to the serious ill-conditioned nature of the problem, from these simulations alone it is not clear whether the developed analysis method is capable of dealing with the statistical error in experimental decays, or if the noise prevents the extraction of the relevant information from decay data.

4. Recovery of Simulated Distributions

Methodology. To answer this question, in the second set of simulations we generated simulated decay curves using the mean local concentration formalism, mostly from synthetic Gaussian and sum-of-two-Gaussian distributions (input), convoluted them with experimental instrumental response functions (for description of the instrumental apparatus, see the following paper), and added Poisson noise. They were then analyzed with our software, returning the output parameters. Both planar and bilayer geometry versions of the programs were tested, and a variety of distributions was generated for each case. Data analysis was carried out using global analysis; i.e., in each case, the synthetic ET decay curve was analyzed together with a synthetic intrinsic decay curve of donor, with linkage of lifetimes and preexponential factors ratio.[20,34] One thousand twenty-four channels were used, and the peak channel count was about 20 000. The linked parameters were set to values close to those of the studied donor probes in the following paper.[6] For the bilayer simulations we used $\tau_1 = 2$ ns, $\tau_2 = 10$ ns, and $q = 1$ in eqs 7−11, and for the planar simulations we used $\tau_1 = 0.8$ ns, $\tau_2 = 3$ ns, and $q = 2$ in eq 6. In the creation of the bilayer decays, the integral in eq 7 was evaluated numerically for each channel, using 500 subintervals for each decay. The time scales were 22 ps/channel for the planar system and 44 ps/channel for the bilayer system. The planar and bilayer simulations gave identical results; for this reason, we only refer to the bilayer simulations throughout this section. In the analysis procedure, at least 200 subintervals were again used to calculate the integrals in eq 7, and c_{max} was chosen as being close to $\max\{c_1 + 4\sigma_1, c_2 + 4\sigma_2\}$.

Results. In Figure 3 are represented the generated and recovered distributions. In Table 2 are represented the χ^2 values for each analysis, as well as the linked parameters for the cases in which their recovery was not correct.

(i) Unimodal Gaussian Distributions. (i.1) Discrete Function. This is the case of homogeneous acceptor distribution. In this case, as expected, program D gives the exact result with good statistics. Programs 1G and 2G also behave well, a narrow distribution being recovered centered around the correct value (Figure 3a).

(i.2) Broad Distribution. Programs 1G and 2G recover distributions close to that used in the simulation with good χ^2 values. Program D, however, returns a c value smaller than the mean distribution value by ∼25%. The lifetimes and especially the preexponential ratio are not correctly recovered, either, and the χ^2 value is not acceptable (Figure 3b).

(ii) Bimodal Gaussian Distributions. Distributions c, d, e, and f are constructed using a sum of two Gaussians, but have quite different shapes. We can distinguish between, on one hand, distributions c and d, which have well separated peaks, and distributions e and f, which have overlapping peaks.

(ii.1) Separated Peaks. For separated peaks, only the program 2G gives good fits, as expected. A model of discrete acceptor concentration could not at all be fitted to the data; a single Gaussian model returns an acceptable χ^2 value for c, the distribution for which the peaks are closer; however, the lifetimes and especially the preexponential ratio are not correctly recovered. Moreover, χ^2 still improves significantly by analyzing with program 2G, with correct values for the linked parameters. Only the relative height of each Gaussian is not correctly recovered (Figure 3c). Distribution d) (Figure 3d) is similar, but now program 1G gives an unacceptable fit, and the recovered function is the tail of a Gaussian. In this case (similarly to cases 3 and 5 in the previous set of simulations) convergence is very slow, because a very broad set of (center of distribution, standard deviation) pairs produces almost identical χ^2 values. For both distributions, the calculated estimates of K_{pA} and the ratio of

TABLE 2: χ^2 Values from Analysis of Synthetic Decay Curves (See Figure 4 for Representation of the Recovered Distributions)

distribution	D (discrete fit)	1G (single Gaussian fit)	2G (sum of Gaussians fit)
(a) discrete	$\chi^2 = 0.981$	$\chi^2 = 0.972$	$\chi^2 = 0.972$
(b) broad symmetric	$\tau_1 = 1.81$ ns, $q = 0.841$ $\tau_2 = 10.27$ ns, $\chi^2 = 2.243$	$\chi^2 = 1.005$	$\chi^2 = 1.002$
(c) bimodal−separated peaks	$\chi^2 > 10$	$\tau_1 = 1.97$ ns, $q = 0.926$ $\tau_2 = 10.13$ ns, $\chi^2 = 1.300$	$\chi^2 = 1.032$ $K_{pA} = 5.0(5.0)$ $N_{1D}/N_{2D} = 0.40(0.17)$
(d) bimodal− separated peaks	$\chi^2 > 10$	$\tau_1 = 1.54$ ns, $q = 1.149$ $\tau_2 = 9.66$ ns, $\chi^2 = 4.288$	$\chi^2 = 1.030$ $K_{pA} = 9.1(8.8)$ $N_{1D}/N_{2D} = 0.26(0.27)$
(e) Gaussian centered at $c = 0$ with a shoulder	$\tau_1 = 1.82$ ns, $q = 0.882$ $\tau_2 = 10.21$ ns, $\chi^2 = 2.058$	$\chi^2 = 1.017$	$\chi^2 = 1.018$
(f) bimodal−overlapping peaks	$q = 0.981$ $\chi^2 = 0.973$	$\chi^2 = 1.035$	$\chi^2 = 1.039$
(g) asymmetric unimodal	$\tau_1 = 1.84$ ns, $q = 0.901$ $\tau_2 = 10.16$ ns, $\chi^2 = 1.847$	$\chi^2 = 0.985$	$\chi^2 = 0.984$

[a] τ_1, τ_2, and q are only represented for the cases when the error in the recovered values was >1% (input values were 2 ns, 10 ns, and 1, respectively). For distributions (c) and (d) the calculated ratios (2G fit) of concentration of acceptor (K_{pA}) and amount of donor (N_{1D}/N_{2D}) in each phase are compared with those of the input distributions (in parentheses).

donors in each environment N_{1D}/N_{2D} agree well with those of the input distributions (see Table 2).

(ii.2) Overlapping Peaks. Distributions e and f (Figures 3e,f, respectively) represent more critical tests to program 2G, since the maxima are not very well defined in e, and the second maximum is reduced to a shoulder in f. Thus, the identification of the Gaussian parameters becomes more difficult. This is indeed the case for e: the program recognizes that there are two distinct peaks (unlike, for example, for distributions a and b, where the two Gaussians merge completely), recovers their location fairly well, but does not get the height and standard deviations right. Program 1G obtains a statistically acceptable fit because the synthetic curve does not deviate considerably from a Gaussian (distinct but unpronounced maxima, almost symmetric curve). Program D fails to return an acceptable χ^2 value because the distribution is broad. However, for distribution f, which is narrower, the fit to a discrete concentration is statistically acceptable. Program 2G predicts the shape of this curve relatively well, except for the shoulder at $c = 0.2$. The fit by program 1G is also good, but requires a negative value for the center of the Gaussian, because in the region of analysis ($0 < c < 1$), the distribution resembles the tail of a Gaussian curve centered on a negative mean value. Indeed, a fit of the distribution f to a single Gaussian $B\exp(-(c-\mu)^2/2\sigma^2)$ (with minimization of the integral of square residuals over $0 < c < 1$) gives $\mu = -0.65$ and $\sigma = 0.32$.

(iii) Asymmetric Unimodal Distribution. So far, we only created synthetic curves from sums of two Gaussians. It could be argued that by analyzing them assuming a sum-of-Gaussians distribution, we are not putting this method to a real challenge. To check whether program 2G could recognize an asymmetric distribution, we created a decay with distribution of acceptor, distribution g, given by the gamma-like distribution $f(c) = 5c\exp(-5c)$ (see Figure 3g). Program D fails to produce a statistically acceptable fit and recovers biased lifetimes and q values. Programs 1G and 2G give statistically acceptable fits; program 1G manages to recover a Gaussian function which emulates relatively well the asymmetric distribution. Program 2G recognizes the distribution asymmetry, failing, however, to recover the correct peak width. This is again a consequence of the ill-conditioned nature of the problem: Not-so-small changes in the parameters produce very small changes in χ^2. In the final stages of the analysis, the direction of the variation of parameters was correct, namely σ_1 was increasing on each iteration. However, the convergence criterion of the program (based on variations of χ^2) was obeyed before a best value could be reached.

5. Discussion

The first set of simulations shows that the mean local concentration model is able to recognize heterogeneity in the distribution of chromophores, provided that the function family used to recover the acceptor concentration distribution is sufficiently flexible, which is the case for the sum of two Gaussians. For heterogeneous samples, the ratio of donor molecules in each phase and the partition coefficient of the acceptor can be estimated. The fact that heterogeneity of probe distribution changes ET efficiency has been widely known for a long time, and was recently illustrated by a Monte Carlo study in which heterogeneity is introduced by a mathematically suitable interaction function.[19] In the present work, heterogeneity is introduced by assuming a phase separated structure in which the continuous phase and the domains have distinct acceptor probe concentrations. This approach is especially adequate to model ET in heterogeneous membranes, e.g., gel/fluid heterogeneity (the "linear phase" structure of simulations 3−5 is relevant to the structure of pure gel phase, as discussed in the following paper). In the simple case of probe homogeneous distribution inside each phase and identical domains, the parameter models are relatively few: the area fraction of the domains, the partition coefficients of the probes, and the size and shape of the domains. The area fraction and partition coefficients are commonly obtained experimentally (e.g., from calorimetric and spectroscopic techniques). Comparison of experimental and Monte Carlo generated decays could thus be used to study the size and shape of the domains. Of course, for domains larger than say, some hundred angstroms, the decay curve is expected to become largely insensitive to the size and shape of the domain. In this case, the comparison can be used to estimate one of the former parameters. In any case, a more systematic Monte Carlo study of the alterations of the decay curve (and the resulting steady-state ET efficiencies) as a function of these parameters in a variety of domain distributions (including different partition of both donors and acceptors and a range of different domain sizes) is in our view relevant per se, and is currently under way.

The second set of simulations provides further insight on the utility and limitations of the analysis programs in conditions identical to typical experiments. We would like to discuss the following aspects.

(1) For discrete distributions, all programs recover a very narrow function, centered on the correct value.

(2) For symmetric unimodal functions, programs 1G and 2G recover the function accurately. Program D fails for broad distributions, giving unacceptable statistics and a significant negative error ($c <$ center of distribution). This agrees with the findings of Golub et al.,[38] who considered the similar but simpler (no need for convolution, exclusively planar system, single lifetime, linear kinetics with respect to time of the Stern−Volmer equation) problem of recovery of simulated distributions of quencher concentration in phosphorescence emission. It is the equivalent of the documented failure in deconvolution of a distribution of lifetimes with a width of ∼20% of its center value by a discrete component.[39]

(3) The simulations of bimodal functions showed that although the exact parameters of the distribution could not be recovered if the peaks overlap, even in this case the general shape of the curve and approximate location of the peaks can be predicted. For nonoverlapping peaks, good estimates of the ratios of concentration of acceptor and number of molecules of donor in each environment are generally obtained. As in (2), Program D fails for broad distributions, while program 1G generally gives good statistics, unless the separation of the peak is large. However, in this case, σ is always large (the recovered Gaussian spreads over the whole c range of the bimodal input curve, see simulation with distribution e).

(4) This last observation illustrates again the ill-conditioned nature of the problem. However, the recovery of a broad Gaussian using program 1G indicates that the distribution might not be unimodal. Therefore, a systematic procedure of analysis of ET data would be to begin by using the single Gaussian model. If a large standard deviation is recovered, say $\sigma \sim 0.3\ \mu$, one should consider repeating the analysis with the sum-of-Gaussians program. This should reveal if the actual distribution is uni- or bimodal. If, on the other hand, a narrow distribution is recovered, say $\sigma \sim 0.1\ \mu$, the discrete model should be adequate. As the simulations with distribution a show, for $\sigma = 0.05\ \mu$ one cannot distinguish a very narrow Gaussian from a homogeneous (discrete function) system. In that case, the discrete analysis is preferred. The standard deviation of the distribution is a measure of its heterogeneity.[38] The narrower the distribution, the closer it can be approximated by the classical discrete concentration model. Because of the ill-conditioned nature of the problem, it is especially crucial to try to increase the precision of the analysis (e.g., using double instead of single precision programming variables, dividing the c analysis range in a large number of intervals, using a smaller χ^2 change as criterion for termination of the analysis), at the expense of speed.

(5) By allowing recovery of a sum of two Gaussians, with varying centers, standard deviations and relative height, we have a class of functions which is capable of fitting a wide range of curves, both symmetric (e.g., Lorentzian, Student's t distributions), and asymmetric (e.g., chi-square, gamma distributions). Simulation g showed that asymmetry could be revealed, at least on a semiquantitative basis. Of course, multipeaked (≥ 3 peaks) distributions may not be fitted too well by a sum of Gaussians, but on one hand, these are highly unlikely to occur (they require at least three different environments of donor molecules), and on the other hand, it would be difficult for any algorithm to recover accurately such a distribution, even for one without a priori assumption of the shape of the distribution, due to the ill-conditioned nature of the problem. In fact, Liu et al. only tested their algorithm (which does not assume the shape of the distribution) on smooth, unimodal curves, except one curve, which was bimodal, but with non overlapping peaks, for which the relative height of the peaks was not accurately recovered.[22] Moreover, from a discrete input function, they recovered a wide distribution, unlike our Gaussian programs. For these input distributions, our sum-of-Gaussians program would probably perform comparably well, with the advantage of still allowing global optimization of two lifetime components and their preexponential ratio. It remains untested if a nonshape-assuming program would behave well for a more complex situation.

(6) In the above simulations, the b parameter, which contains information on the bilayer width (or, more precisely, the distance between the plane of the donors in one leaflet and the plane of the acceptors in the other leaflet) was always kept constant. We found that χ^2 was relatively insensitive to this parameter for a b value of $\sim 1\ \mathrm{ns}^{-1/3}$ or less. This is because transfer between chromophores of opposing leaflets, while being sufficiently important so as to not be neglected, is much weaker than that within the same leaflet.[3] Additionally, the optimization of b would imply the calculation of the integral in eq 9 for each iteration, which would slow the program considerably. Therefore, in the analysis of experimental curves in the following paper, we do not optimize b, but fix it to a value calculated from independent methods instead.

6. Conclusions

The mean local concentration model, with a sum-of-two-Gaussians as the acceptor concentration distribution function, is shown to describe adequately simulated heterogeneous ET decays in two-dimensional and bilayer geometries. It is possible to recover important information, such as partition coefficients of the probes. Even upon adding noise, the programs, namely the 2G version, are able to differentiate between narrow and wide, unimodal and bimodal, and symmetric and asymmetric distributions. Because of ill-conditioning and/or parameter correlation, complete quantification is sometimes impossible in noisy samples. For example, it is not always possible to distinguish between a sharp, relatively high peak and a broad, lower peak in a bimodal distribution. Other unfavorable cases are those of peak overlapping or distribution asymmetry. In any case, however difficult it might be to recover the exact or closest available distributions, the general shape, approximate width, and approximate peak locations and relative weights are well recovered. This formalism, which is applied to probe distribution heterogeneity in pure lipid vesicles in the following paper, is especially suited to the study of gel/fluid membrane heterogeneity, and other similar topological information in membranes.

Acknowledgment. This work was supported by PRAXIS XXI (M.C.T., Portugal), Project PRAXIS/P/SAU/14025/1998. Profs. J. M G. Martinho and M. N. Berberan-Santos are gratefully acknowledged for a critical reading of the manuscript.

References and Notes

(1) Stryer, L.; Haugland, R. P. *Proc. Natl. Acad. Sci. U.S.A.* **1967**, *58*, 716.

(2) For a review, see: Wu, P.; Brand, L. *Anal. Biochem.* **1994**, *218*, 1.

(3) Fung, B. K.-K.; Stryer, L. *Biochemistry* **1978**, *17*, 5241.

(4) Davenport, L.; Dale, R. E.; Bisby, R. H.; Cundall, R. B. *Biochemistry* **1985**, *24*, 4097.

(5) Tamai, N.; Yamazaki, T.; Yamazaki, I.; Mizuma, A.; Mataga, N. *J. Phys. Chem.* **1987**, *91*, 3503.
(6) Loura, L. M. S.; Fedorov, A.; Prieto, M. *J. Phys. Chem B* **2000**, *104*, 6920.
(7) Klafter, J.; Blumen, A. *J. Chem. Phys.* **1984**, *80*, 875.
(8) Hauser, M.; Klein, U. K. A.; Gösele, U. *Z. Phys. Chem.* **1976**, *101*, 255.
(9) Rojanski, D.; Huppert, D.; Bale, H. D.; Dacai, X.; Schmidt, P. W.; Farin, D.; Seri-Levy, A.; Avnir, D. *Phys. Rev. Lett.* **1986**, *56*, 2505.
(10) Even, U.; Rademann, K.; Jortner, J.; Manor, N.; Reisfeld, E. *Phys. Rev. Lett.* **1984**, *52*, 2164.
(11) Yamazaki, I.; Tamai, N.; Yamazaki, T. **1987**. *J. Phys. Chem. 91*, 3572.
(12) Ohta, N.; Tamai, T.; Kuroda, T.; Yamazaki, T.; Nishimura, Y.; Yamazaki, I. *Chem. Phys.* **1993**, *177*, 591.
(13) Yang, C. L.; Evesque, P.; El-Sayed, M. A. *J. Phys. Chem.* **1985**, *89*, 3442.
(14) Klafter, J.; Blumen, A. *J. Lumin.* **1985**, *34*, 77.
(15) Blumen, A.; Klafter, J.; Zumofen, G. *J. Chem. Phys.* **1986**, *84*, 1397.
(16) Levitz, P.; Drake, J. M. *Phys. Rev. Lett.* **1987**, *58*, 686.
(17) Levitz, P.; Drake, J. M.; Klafter, J. *J. Chem. Phys.* **1988**, *89*, 5224.
(18) Pekcan, Ö.; Egan, L. S.; Winnik, M. A.; Croucher, M. D. *Macromolecules* **1990**, *23*, 2210.
(19) Barbosa-Garcia, O.; Struck, C. W. *J. Chem. Phys.* **1994**, *100*, 4554.
(20) Loura, L. M. S.; Fedorov, A.; Prieto, M. *Biophys. J.* **1996**, *71*, 1823.
(21) Ballet, P.; Van der Auweraer, M.; De Schryver, F. C.; Lemmetyinen, H.; Vuorimaa, E. *J. Phys. Chem.* **1996**, *100*, 13701.
(22) Liu, Y. S.; Li, L.; Ni, S.; Winnik, M. A. *Chem. Phys.* **1993**, *177*, 579.
(23) Liu, Y. S.; Feng, J.; Winnik, M. A. *J. Chem. Phys.* **1994**, *101*, 9096.
(24) Dhinojwala, A.; Torkelson, J. M. *Macromolecules* **1994**, *27*, 4817.
(25) Deppe, D. D.; Dhinojwala, A.; Torkelson, J. M. *Macromolecules* **1996**, *29*, 3898.
(26) Yetka, A.; Duhamel, J.; Winnik, M. A. *Chem. Phys. Lett.* **1995**, *235*, 119.
(27) Farinha, J. P. S.; Martinho, J. M. G.; Yekta, A.; Winnik, M. A. *Macromolecules* **1995**, *28*, 6084.
(28) Farinha, J. P. S.; Martinho, J. M. G.; Kawaguchi, S.; Yetka, A.; Winnik, M. A. *J. Phys. Chem.* **1996**, *100*, 12552.
(29) Barzykin, A. V.; Tachiya, M. *Macromolecules* **1996**, *29*, 6351.
(30) For a review, see Ware, W. R. In *Photochemistry in Organized and Constrained Media*; Ramamurthy, V., Ed.; VCH: New York, 1991; 563.
(31) Cantor, C. R.; Pechukas, P. *Proc. Natl. Acad. Sci. U.S.A.* **1971**, *68*, 2099.
(32) Amir, D.; Haas, E. *Biochemistry* **1987**, *26*, 2162.
(33) Lakowicz, J. R.; Gryczynski, I.; Cheung, H. C.; Wang, C.-K.; Johnson, M. L.; Joshi, N. *Biochemistry* **1988**, *27*, 9149.
(34) Beechem, J. M.; Gratton, E.; Ameloot, M.; Knutson, J. R.; Brand, L. In *Topics in Fluorescence Spectroscopy, Volume 2: Principles*; Lakowicz, J. R., Ed.; Plenum: New York, 1991; 241.
(35) Förster, Th. *Z. Naturforsch.* **1949**, *4a*, 327.
(36) Snyder, B. Freire, E. *Biophys. J.* **1982**, *40*, 137.
(37) Marquardt, D. W. *J. Soc. Ind. Appl. Math. (SIAM J.)* **1963**, *11*, 431.
(38) Golub, A. S.; Popel, A. S.; Zheng, L.; Pittman, R. N. *Biophys. J.* **1997**, *73*, 452.
(39) Vix, A.; Lami, H. *Biophys. J.* **1995**, *68*, 1145.